Supporting Information for

# Resolving Mixed Intermediate Phases in Methylammonium-Free Sn-Pb Alloyed Perovskites for High-Performance Solar Cells

Zhanfei Zhang[1], Jianghu Liang[1], Jianli Wang[1], Yiting Zheng[1], Xueyun Wu[1], Congcong Tian[1], Anxin Sun[1], Zhenhua Chen[2], Chun-Chao Chen[1, *]

[1]School of Materials Science and Engineering, Shanghai Jiao Tong University, Shanghai 20024, P. R. China

[2]Shanghai Synchrotron Radiation Facility (SSRF), Shanghai Advanced Research Institute, Chinese Academy of Sciences, Shanghai 201800, P. R. China

*Corresponding author. E-mail: c3chen@sjtu.edu.cn (Chun-Chao Chen)

## Supplementary Figures

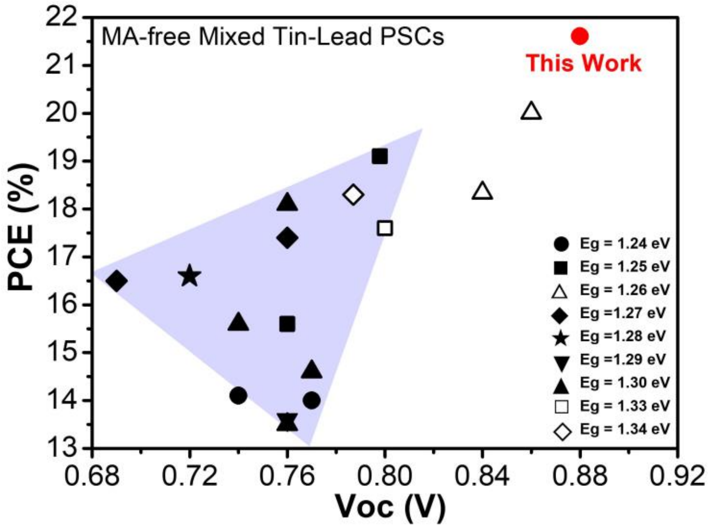


**Fig. S1** Efficiencies of previously reported MA-free Pb–Sn alloyed PSCs, plotted with their the band gaps ($E_g$). All references for this figure are given in **Table S1**

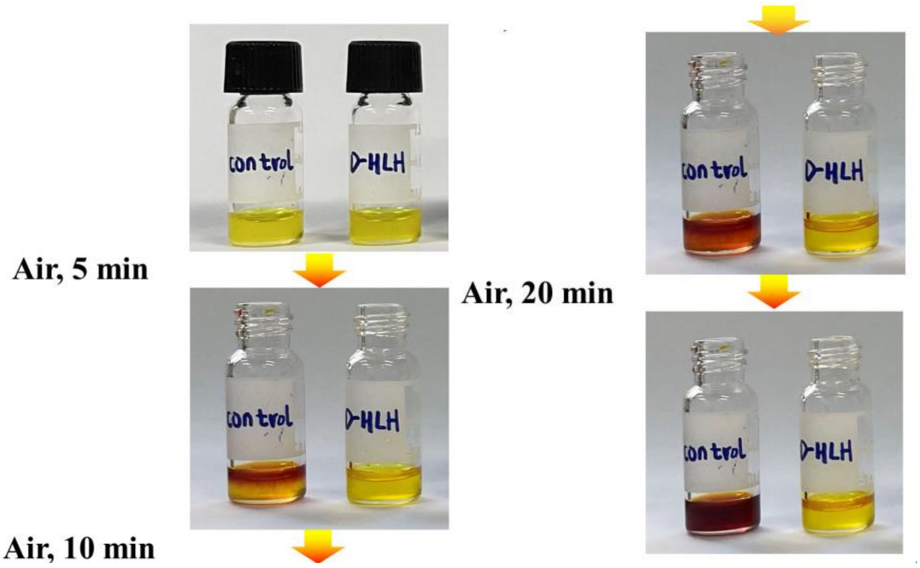


**Fig. S2** Photographs of $Cs_{0.25}FA_{0.75}Pb_{0.6}Sn_{0.4}I_3$ perovskite precursor solutions, prepared with or without D-HLH, after exposure to the air for up to 20 min

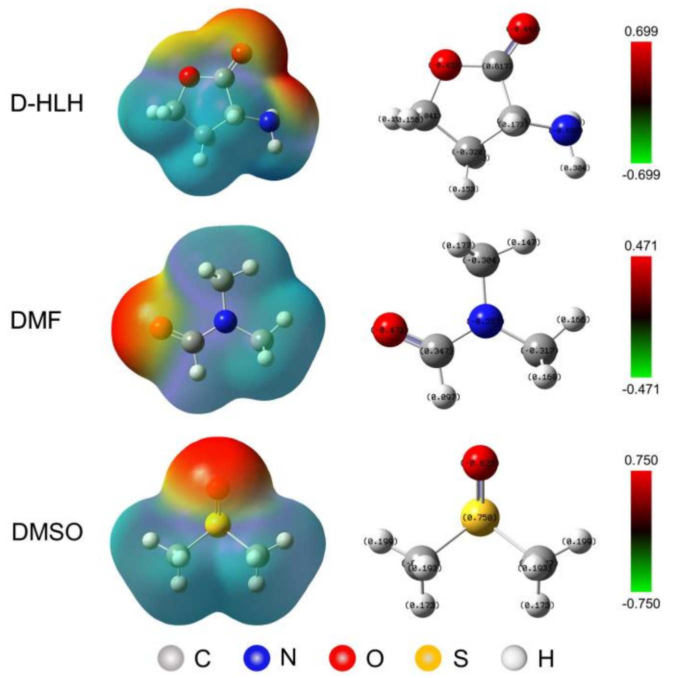


**Fig. S3** (**left**) Electrostatic potentials and (**right**) charge distributions of D-HLH, DMF, and DMSO

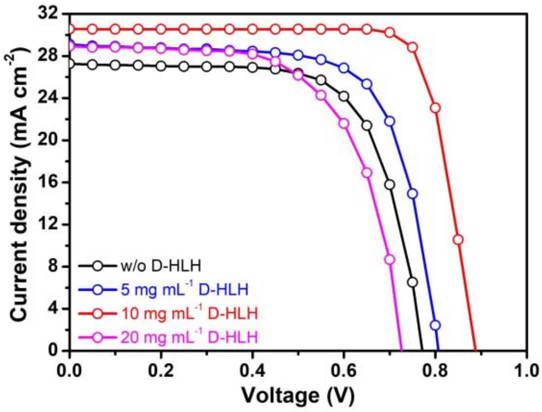


**Fig. S4** *J*–*V* curves of PSCs prepared using different concentrations of D-HLH

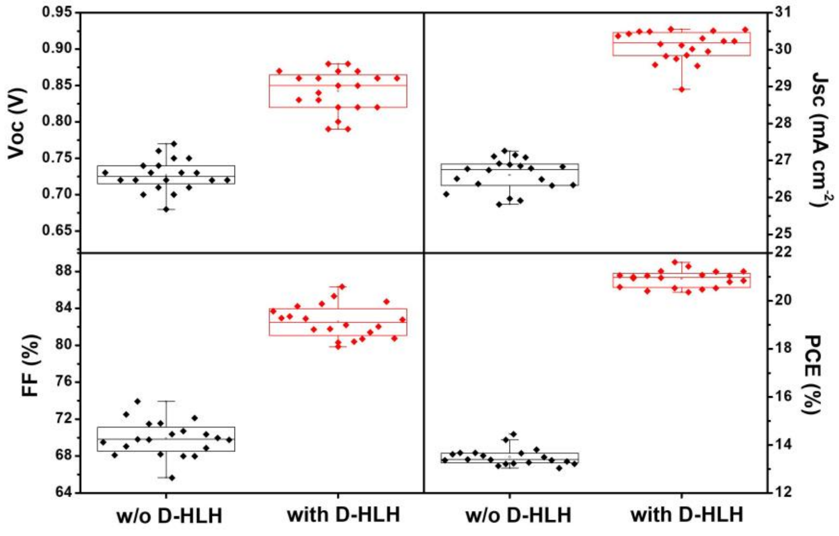


**Fig. S5** Statistics of the values of $V_{oc}$, $J_{sc}$, FF, and PCE from 20 devices containing the control and D-HLH–treated perovskites

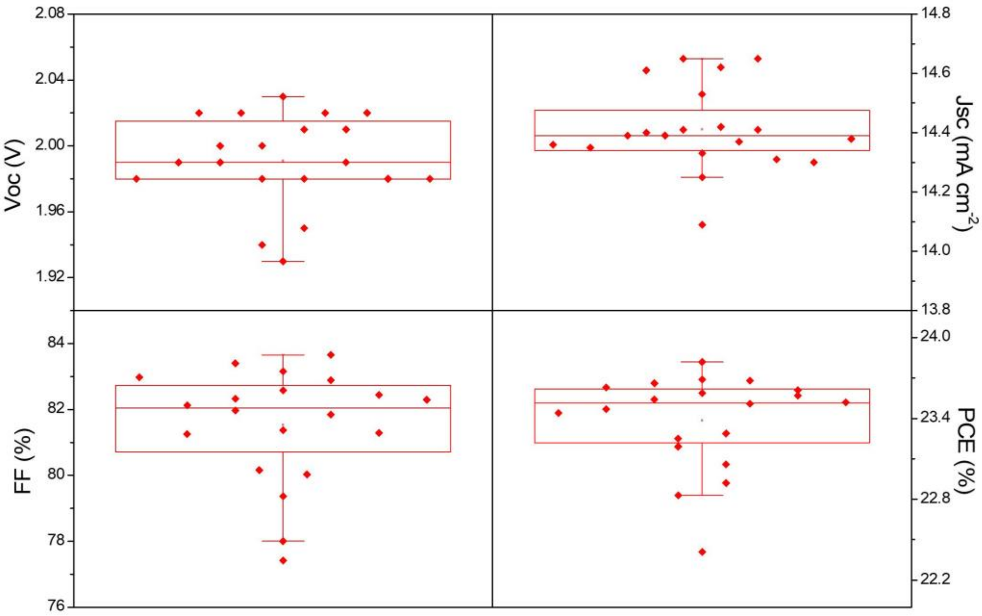


**Fig. S6** Statistics of the values of $V_{oc}$, $J_{sc}$, FF, and PCE from 20 tandem devices prepared with D-HLH treatment

**Table S1** Performance data of reported highly efficient MA-free Pb–Sn alloyed PSCs

| **Perovskite** | ***E*$_g$ (eV)** | ***V*$_{oc}$ (V)** | ***J*$_{sc}$ (mA cm$^{-2}$)** | **FF (%)** | **PCE (%)** | **Stability** | | | **Refs.** |
|---|---|---|---|---|---|---|---|---|---|
| | | | | | | Thermal (85 °C) | Light (MPP*) | Storage ($N_2$) | |
| $Cs_{0.25}FA_{0.75}Pb_{0.5}Sn_{0.5}I_3$ | 1.24 | 0.74 | 26.7 | 71 | 14.1 | 70 h, 40%; 1500 h, 30% | 50 min, 90% | – | [S1] |
| $Cs_{0.2}FA_{0.8}Sn_{0.5}Pb_{0.5}I_3$ | 1.24 | 0.77 | 25.6 | 69 | 14.0 | | | | |
| $Cs_{0.15}FA_{0.85}Sn_{0.625}Pb_{0.375}I_3$ | 1.26 | 0.76 | 24.6 | 70 | 13.5 | | | | |
| $Cs_{0.225}FA_{0.775}Sn_{0.625}Pb_{0.375}I_3$ | 1.28 | 0.76 | 25.6 | 72 | 13.6 | – | – | – | [S2] |
| $Cs_{0.2}FA_{0.8}Sn_{0.7}Pb_{0.3}I_3$ | 1.30 | 0.76 | 25.1 | 76 | 13.5 | | | | |
| $Cs_{0.3}FA_{0.7}Pb_{0.7}Sn_{0.3}I_3$ | 1.30 | 0.77 | 26.4 | 71.6 | 14.6 | – | – | – | [S3] |
| $Cs_{0.25}FA_{0.75}Pb_{0.5}Sn_{0.5}I_3$ | 1.25 | 0.76 | 27.6 | 74 | 15.6 | 325 h, 82% | 30 h, 100% | – | [S4] |
| $Cs_{0.3}FA_{0.7}Pb_{0.7}Sn_{0.3}I_3$ | 1.30 | 0.74 | 25.89 | 81.4 | 15.6 | – | – | 288 h, 98.3% | [S5] |
| $Cs_{0.25}FA_{0.75}Sn_{0.5}Pb_{0.5}I_3$ | 1.29 | 0.72 | 30.8 | 74.95 | 16.6 | 600 h, 50% | 1000 h, 90% | – | [S6] |
| $Cs_{0.25}FA_{0.75}Sn_{0.5}Pb_{0.5}I_3$ | 1.27 | 0.69 | 31.7 | 76 | 16.5 | – | – | – | [S7] |
| $Cs_{0.15}FA_{0.85}Sn_{0.3}Pb_{0.7}I_3$ | 1.33 | 0.80 | 28.7 | 73.5 | 17.6 | – | – | – | [S8] |
| $Cs_{0.15}FA_{0.85}Sn_{0.5}Pb_{0.5}I_3$ | 1.30 | 0.76 | 30.3 | 78.3 | 18.1 | | | | |
| $Cs_{0.25}FA_{0.75}Sn_{0.5}Pb_{0.5}I_3$ | 1.25 | 0.798 | 31.1 | 78.4 | 19.1 | 4000 h, 80% | – | – | [S9] |
| $Cs_{0.15}FA_{0.85}Sn_{0.5}Pb_{0.5}I_3$ | 1.27 | 0.76 | 31.3 | 73 | 17.4 | – | – | 300 h, air, 65% | [S10] |
| $Cs_{0.3}FA_{0.7}Sn_{0.3}Pb_{0.7}I_3$ | 1.34 | 0.787 | 29.1 | 79.9 | 18.3 | – | 750 h, 80% | – | [S11] |
| GDR-$Pb^0$ (8.5) | 1.26 | 0.84 | 30.37 | 72.24 | 18.34 | – | 700 h, 80% | 2352 h, $N_2$, 81% | [S12] |
| GDR-$Pb^0$ (18.7) | | 0.86 | 31.55 | 73.64 | 20.01 | – | – | – | |
| $Cs_{0.2}FA_{0.8}Pb_{0.5}Sn_{0.5}I_3$ | 1.24 | 0.86 | 31.5 | 77.9 | 21.10 | – | – | – | [S13] |

*MPP: continuous operation stability with maximum power point (MPP) tracking under 1-sun illumination.

**Table S2** Peak parameters and assignments of Pb 4f and Sn 3d XPS signals for perovskites prepared with or without additive doping

| Elements | Binding Energy (eV) | Sample | Affiliation |
| --- | --- | --- | --- |
| Pb | 137.98/142.88[a)] | Control | **Pb** in PbO[S14–S18], $Pb_3O_4$[S19, S20], Pb[S20], and PbS[S21] |
| | 137.78/142.68[a)] | D-HLH | **Pb** in PbO[S22–S27], and PbS[S21, S22, S28] |
| Sn | 487.28/495.68[b)] | Control | **Sn** in $SnO_2$[S29–S31], $SnO_{1.65}$[S31], $SnCl_2$[S32], $SnF(C_6H_5)_3$[S33], $Sn(C_6H_5)_2Cl_2$[S34], $SnCl_4(C_5H_5N)_2$[S35], $SnCl_3(C_2H_5)(C_5H_5N)_2$[S35], and $SnCl_3(C_6H_5)(C_5H_5N)_2$[S35] |
| | 487.08/495.48[b)] | D-HLH | **Sn** in SnO[S20, S36], $SnF_2$[S20, S37], $SnO_2$[S30, S31, S38–S40], $SnO_{1.65}$[S31], $SnF_2(CH_3)_2$[S35], $Sn(CH_3)_2SO_4$[S35], $SnCl(C_6H_5)_3$[S20], $Sn(C_6H_5)_4$[S35], $SnCl_2(CH_3)_2(SO(CH_3)_2)_2$[S35], and $Sn(C_6H_5)_3(C_9H_6NO)$[S41] |

a) Pb $4f_{7/2}/4f_{5/2}$; b) Sn $3d_{5/2}/3d_{3/2}$

**Table S3** Peak parameters and assignments of O 1s XPS signals for perovskites prepared with and without additive doping

| Sample | O in inorganic molecule | | | O in organic molecule | | |
| --- | --- | --- | --- | --- | --- | --- |
| | Binding energy (eV) | FWHM [c)] (eV) | Atomic ratio (%) | Binding energy (eV) | FWHM [c)] (eV) | Atomic ratio (%) |
| Control | 530.96[S40, S42] | 1.63 | 46 | 532.21[S43, S44] | 1.90 | 54 |
| D-HLH | 530.62[S45, S46] | 1.60 | 27 | 531.82[S47, S48, S49–S62] | 2.19 | 73 |

c) Full width at half maximum.

**Table S4** FTIR spectral data for perovskites prepared with and without additive doping

| Sample | Wavenumber ($cm^{-1}$) | | |
| --- | --- | --- | --- |
| | N–H stretching | | C=O stretching |
| Control | 3411 | 3270 | 1633 |
| D-HLH | 3401 | 3231 | 1607 |

**Table S5** Photovoltaic parameters of PSCs prepared using different concentrations of D-HLH

| D-HLH concentration (mg $mL^{-1}$) | $V_{oc}$ (V) | $J_{sc}$ (mA $cm^{-2}$) | FF (%) | PCE (%) |
| --- | --- | --- | --- | --- |
| 5 | 0.81 | 29.10 | 69.89 | 16.47 |
| 10 | 0.88 | 30.56 | 80.36 | 21.61 |
| 20 | 0.72 | 28.93 | 64.04 | 13.34 |

**Table S6** Photovoltaic parameters of champion PSCs prepared with and without D-HLH

| Device | Scan | $V_{oc}$ (V) | $J_{sc}$ (mA $cm^{-2}$) | FF (%) | PCE (%) | Integrated $J_{sc}$ (mA $cm^{-2}$) |
| --- | --- | --- | --- | --- | --- | --- |
| Control | Reverse | 0.77 | 27.26 | 69.13 | 14.51 | 27.12 |
| | Forward | 0.76 | 27.41 | 67.54 | 14.07 | |
| D-HLH | Reverse | 0.88 | 30.56 | 80.36 | 21.61 | 29.86 |
| | Forward | 0.88 | 30.55 | 78.26 | 21.04 | |

**Table S7** Photovoltaic parameters of champion tandem devices prepared with D-HLH

| Device | Scan | $V_{oc}$ (V) | $J_{sc}$ (mA cm$^{-2}$) | FF (%) | PCE (%) |
|---|---|---|---|---|---|
| Front cell | Reverse | 1.18 | 16.21 | 82.15 | 15.71 |
| | Forward | 1.18 | 16.19 | 81.61 | 15.59 |
| Back cell | Reverse | 0.88 | 30.56 | 80.36 | 21.61 |
| | Forward | 0.88 | 30.55 | 78.26 | 21.04 |
| Tandem-D-HLH | Reverse | 2.03 | 14.42 | 81.37 | 23.82 |
| | Forward | 2.03 | 14.32 | 81.12 | 23.58 |

**Table S8** Fitting parameters for TRPL curves of perovskite films

| Sample | $\tau_{avg}$ (ns) | $\tau_1$ (ns) | $\tau_2$ (ns) | $A_1$ (%) | $A_2$ (%) |
|---|---|---|---|---|---|
| Control | 9.14 | 1.77 | 13.44 | 81.58 | 18.42 |
| D-HLH | 28.81 | 3.39 | 31.93 | 53.67 | 46.33 |

$F(t) = A_1\exp(-t/\tau_1) + A_2\exp(-t/\tau_2) + y_0$

where $\tau_1$ and $\tau_2$ are the fast and slow decay times, respectively, and $A_1$ and $A_2$ are coefficients.

**Table S9** Related parameters fitted from the equivalent circuit for EIS spectral measurement

| Device | $R_s$ (Ω) | $R_{ct}$ (Ω) | $C$ (nF) | $R_{rec}$ (Ω) | CPE (nF) |
|---|---|---|---|---|---|
| Control | 60.11 | 20,210 | 15 | 14,560 | 3970 |
| D-HLH | 42.06 | 3384 | 7783 | 19,220 | 28.21 |

## Supplementary References


[S1] G.E. Eperon, T. Leijtens, K.A. Bush, R. Prasanna, T. Green et al., Perovskite-perovskite tandem photovoltaics with optimized band gaps. Science **354**(6314), 861–865 (2021). https://doi.org/10.1126/science.aaf9717

[S2] R. Prasanna, A. Gold-Parker, T. Leijtens, B. Conings, A. Babayigit et al., Band gap tuning via lattice contraction and octahedral tilting in perovskite materials for photovoltaics. J. Am. Chem. Soc. **139**(32), 11117–11124 (2021). https://doi.org/10.1021/jacs.7b04981

[S3] Y. Zong, N. Wang, L. Zhang, M.G. Ju, X.C. Zeng et al., Homogenous alloys of formamidinium lead triiodide and cesium tin triiodide for efficient ideal-bandgap perovskite solar cells. Angew. Chem. Int. Ed. **56**(41), 12658–12662 (2021). https://doi.org/10.1002/anie.201705965

[S4] T. Leijtens, R. Prasanna, K.A. Bush, G.E. Eperon, J.A. Raiford et al., Tin–lead halide perovskites with improved thermal and air stability for efficient all-perovskite tandem solar cells. Sustain. Energy Fuels **2**(11), 2450–2459 (2021). https://doi.org/10.1039/C8SE00314A

[S5] Y. Zong, Z. Zhou, M. Chen, N.P. Padture, Y. Zhou, Lewis-adduct mediated grain-boundary functionalization for efficient ideal-bandgap perovskite solar cells with superior stability. Adv. Energy Mater. **8**(27), 1800997 (2021). https://doi.org/10.1002/AENM.201800997

[S6] R. Prasanna, T. Leijtens, S.P. Dunfield, J.A. Raiford, E.J. Wolf et al., Design of low bandgap tin–lead halide perovskite solar cells to achieve thermal, atmospheric and operational stability. Nat. Energy **4**(11), 939–947 (2021). https://doi.org/10.1038/s41560-019-0471-6

[S7] A.F. Palmstrom, G.E. Eperon, T. Leijtens, R. Prasanna, S.N. Habisreutinger et al., Enabling flexible all-perovskite tandem solar cells. Joule **3**(9), 2193–2204 (2019). https://doi.org/10.1016/j.joule.2019.05.009

[S8] M.T. Klug, R.L. Milot, R.L. Milot, J.B. Patel, T. Green et al., Metal composition influences optoelectronic quality in mixed-metal lead–tin triiodide perovskite solar absorbers. Energy Environ. Sci. **13**(6), 1776–1787 (2021). https://doi.org/10.1039/D0EE00132E

[S9] J. Werner, T. Moot, T.A. Gossett, I.E. Gould, A.F. Palmstrom et al., Improving low-bandgap tin-lead perovskite solar cells via contact engineering and gas quench processing. ACS Energy Lett. **5**(4), 1215–1223 (2021). https://doi.org/10.1021/acsenergylett.0c00255

[S10] H. Liu, J. Sun, H. Hu, Y. Li, B. Hu et al., Antioxidation and energy-level alignment for improving efficiency and stability of hole transport layer-free and methylammonium-free tin-lead perovskite solar cells. ACS Appl. Mater. Interfaces **13**(37), 45059–45067 (2021). https://doi.org/10.1021/acsami.1c12180

[S11] J. Tong, J. Gong, M. Hu, S.K. Yadavalli, Z. Dai et al., High-performance methylammonium-free ideal-band-gap perovskite solar cells. Matter **4**(4), 1365–1376 (2021). https://doi.org/10.1016/J.MATT.2021.01.003

[S12] W. Zhang, X. Li, S. Fu, X. Zhao, X. Feng et al., Lead-lean and MA-free perovskite solar cells with an efficiency over 20%. Joule **5**, 2904-1914 (2021). https://doi.org/10.1016/j.joule.2021.09.008

[S13] Z. Yu, X. Chen, S.P. Harvey, Z. Ni, B. Chen et al., Gradient doping in Sn–Pb perovskites by barium ions for efficient single-junction and tandem solar cells. Adv. Mater., (2022). https://doi.org/10.1002/adma.202110351

[S14] J.M. Baker, R.W. Johnson, R.A. Pollak, Surface analysis of rf plasma oxidized in and PbInAu films using esca. J. Vac. Sci. Technol. **16**(5), 1534–1541 (1979). https://doi.org/10.1116/1.570243

[S15] C. Hinnen, C.N. Huong, P. Marcus, A comparative X-ray photoemission study of $Bi_2Sr_2CaCu_2O_8^{+\delta}$ and $Bi_{1.6}Pb_{0.4}Sr_2CaCu_2O_8^{+\delta'}$. J. Electron Spectros. Relat. Phenomena **73**(3), 293–304 (1995). https://doi.org/10.1016/0368-2048(94)02288-7

[S16] H. Kanai, M. Yoshiki, M. Hayashi, R. Kuwae, Y. Yamashita, Grain-boundary-phase identification of a lead-based relaxor by X-ray photoelectron spectroscopy. J. Am. Ceram. Soc. **77**(8), 2229–2231 (1994). https://doi.org/10.1111/j.1151-2916.1994.tb07128.x

[S17] G. Gökagaç, B.J. Kennedy, Potential-dependent surface segregation in lead + ruthenium pyrochlore $Pb_2Ru_2O_{7-y}$. J. Electroanal. Chem. **353**(1–2), 71–80 (1993). https://doi.org/10.1016/0022-0728(93)80287-R

[S18] P.A. Bertrand, P.D. Fleischauer, X-Ray photoelectron spectroscopy study of the surface adsorption of lead naphthenate. J. Vac. Sci. Technol. **17**(6), 1309–1314 (1980). https://doi.org/10.1116/1.570661

[S19] C. Barriga, S. Maffi, L.P. Bicelli, C. Malitesta, Electrochemical lithiation of $Pb_3O_4$. J. Power Sources **34**(4), 353–367 (1991). https://doi.org/10.1016/0378-7753(91)80101-3

[S20] W.E. Morgan, J.R.V. Wazer, Binding energy shifts in the X-ray photoelectron spectra of a series of related group IVa compounds. J. Phys. Chem. **77**(7), 964–969 (1973). https://doi.org/10.1021/J100626A023

[S21] A.R.H.F. Ettema, C. Haas, An X-ray photoemission spectroscopy study of interlayer charge transfer in some misfit layer compounds. J. Phys. Condens. Matter **5**(23), 3817–3826 (1993). https://doi.org/10.1088/0953-8984/5/23/008

[S22] D.S. Zingg, D.M. Hercules, D.M. Hercules, Electron spectroscopy for chemical analysis studies of lead sulfide oxidation. J. Phys. Chem. **82**(18), 1992–1995 (1978). https://doi.org/10.1021/j100507a008

[S23] V.I. Nefedov, M.N. Firsov, I.S. Shaplygin, Electronic structures of $MRhO_2$, $MRh_2O_4$, $RhMO_4$ and $Rh_2MO_6$ on the basis of X-ray spectroscopy and ESCA data. J. Electron Spectros. Relat. Phenomena **26**(1), 65–78 (2021). https://doi.org/10.1016/0368-2048(82)87006-0

[S24] L.R. Pederson, Two-dimensional chemical-state plot for lead using XPS. J. Electron Spectros. Relat. Phenomena **28**(2), 203–209 (2021). https://doi.org/10.1016/0368-2048(82)85043-3

[S25] J.A. Taylor, D.L. Perry, An X-ray photoelectron and electron energy loss study of the oxidation of lead. J. Vac. Sci. Technol. A **2**(2), 771–774 (2021). https://doi.org/10.1116/1.572569

[S26] J.F. Moulder, W.F. Stickle, P.E. Sobol, K.D. Bomben, *Handbook of X-ray Photoelectron Spectroscopy: A Reference Book of Standard Spectra for Identification and Interpretation of XPS Data*. Physical Electronics Division, Perkin-Elmer Corporation, (1992).

[S27] O. Sakurada, M. Taga, H. Takahashi, X-ray photoelectron spectroscopic study of the stabilization of lead with a palladium modifier in graphite furnace aas. Bunseki Kagaku **38**(9), 407–412(2021). https://doi.org/10.2116/bunsekikagaku.38.9_407

[S28] K. Laajalehto, I. Kartio, P. Nowak, XPS study of clean metal sulfide surfaces. Appl. Surf. Sci. **81**(1), 11–15 (1994). https://doi.org/10.1016/0169-4332(94)90080-9

[S29] Ş. Süzer, T. Voscoboinikov, K.R. Hallam, G.C. Allen, Electron spectroscopic investigation of Sn coatings on glasses. Fresenius J. Anal. Chem. **355**(5), 654–656 (1996). https://doi.org/10.1007/S00216663550654

[S30] M.A. Stranick, A. Moskwa, $SnO_2$ by XPS. Surf. Sci. Spectra **2**(1), 50–54 (1993). https://doi.org/10.1116/1.1247724

[S31] W. Choi, H. Jung, S. Koh, Chemical shifts and optical properties of tin oxide films grown by a reactive ion assisted deposition. J. Vac. Sci. Technol. **14**(2), 359–366 (1996). https://doi.org/10.1116/1.579901

[S32] G.T. Baronetti, S.R. Miguel, O.A. Scelza, A.A. Castro, State of metallic phase in $PtSn/Al_2O_3$ catalysts prepared by different deposition techniques. Appl. Catal. **24**(1–2), 109–116 (1986). https://doi.org/10.1016/S0166-9834(00)81261-0

[S33] S. Hoste, D.F. Vondel, G.P. Kelen, XPS Spectra of organometallic phenyl compounds of P, As, Sb and Bi. J. Electron Spectros. Relat. Phenomena **17**(3), 191–195 (1979). https://doi.org/10.1016/0368-2048(79)85040-9

[S34] M. Andersson, J. Blomquist, B. Folkesson, R. Larsson, P. Sundberg, Esca, mössbauer and infrared spectroscopic investigations of a series of tin complexes. J. Electron Spectros. Relat. Phenomena **40**(4), 385–396 (1986). https://doi.org/10.1016/0368-2048(86)80047-0

[S35] H. Willemen, D.F. Vondel, G.P. Kelen, An ESCA study of tin compounds. Inorg. Chim. Acta **34**, 175–180 (1979). https://doi.org/10.1016/S0020-1693(00)94698-X

[S36] J.C.C. Fan, J.B. Goodenough, X-ray photoemission spectroscopy studies of Sn-doped indium-oxide films. J. Appl. Phys. **48**(8), 3524–3531 (1977). https://doi.org/10.1063/1.324149

[S37] P. Owens, P.A. Grutsch, V. Zeller, T.P. Fehlner, K. Siegbahn et al., Photoelectron spectroscopy of tin compounds. Acta Crystallogr. Sect. B **12**(6), 1431–1433 (1973). https://doi.org/10.1021/ic50124a045

[S38] S. Badrinarayanan, A.B. Mandale, V.G. Gunjikar, A.P.B. Sinha, Mechanism of high-temperature oxidation of tin selenide. J. Mater. Sci. **21**(9), 3333–3338 (1986). https://doi.org/10.1007/BF00553376

[S39] E. Çetinörgü, S. Goldsmith, Y. Rosenberg, R.L. Boxman, Influence of annealing on the physical properties of filtered vacuum arc deposited tin oxide thin films. J. Non. Cryst. Solids **353**(26), 2595–2602 (1996). https://doi.org/10.1016/j.jnoncrysol.2007.04.031

[S40] M.D. Giulio, G. Micocci, A. Serra, A. Tepore, R. Rella et al., $SnO_2$ thin films for gas sensor prepared by r.f. reactive sputtering. Sens. Actuat. B Chem. **25**(1–3), 465–468 (1995). https://doi.org/10.1016/0925-4005(94)01397-7

[S41] P. Umapathy, S. Badrinarayanan, A.P.B. Sinha, An ESCA study of tin (IV) and tin (II) chelates with substituted 8-quinolinols. J. Electron Spectros. Relat. Phenomena **28**(3), 261–266 (1983). https://doi.org/10.1016/0368-2048(83)80004-8

[S42] M.D. Giulio, A. Serra, A. Tepore, R. Rella, P. Siciliano et al., Influence of the deposition parameters on the physical properties of tin oxide thin films. Mater. Sci. Forum **203**, 143–148 (1996). https://doi.org/10.4028/www.scientific.net/msf.203.143

[S43] C.M. Barnes, B.J. Kennedy, An X-ray photoelectron spectroscopic study of arene chromium tricarbonyl complexes at 170K. J. Mol. Struct. **344**(3), 233–240 (1995). https://doi.org/10.1016/0022-2860(95)08461-4

[S44] G. Beamson, D. Briggs, High Resolution XPS of organic polymers: the scienta ESCA300 database. J. Chem. Educ. **70**(1), A25 (1993). https://doi.org/10.1021/ed070pa25.5

[S45] P.R. Moses, H.O. Finklea, J.R. Lenhard, R.W. Murray, L.M. Wier et al., X-ray photoelectron spectroscopy of alkylamine-silanes bound to metal oxide electrodes. Anal. Chem. **50**(4), 576–585 (1978). https://doi.org/10.1021/ac50026a010

[S46] W. Choi, H. Jung, S. Koh, Chemical shifts and optical properties of tin oxide films grown by a reactive ion assisted deposition. J. Vac. Sci. Technol. **14**(2), 359–366 (1996). https://doi.org/10.1116/1.579901

[S47] H. Binder, D. Sellmann, Röntgen-photoelektronenspektroskopische untersuchungen an pentacarbonyl- chrom-und -wolfram-komplexen mit stickstoffliganden / X-ray photoelectron studies of pentacarbonyl chromium and tungsten complexes with nitrogen ligands. Zeitschrift Für Naturforsch. B **33**(2), 173–179 (1978). https://doi.org/10.1515/ZNB-1978-0211

[S48] S. Srivastava, S. Badrinarayanan, A.J. Mukhedkar, X-ray photoelectron spectra of metal complexes of substituted 2,4-pentanediones. Polyhedron **4**(3), 409–414 (1985). https://doi.org/10.1016/S0277-5387(00)87000-X

[S49] C.D. Wagner, D.A. Zatko, R.H. Raymond, Use of the oxygen KLL auger lines in identification of surface chemical states by electron spectroscopy for chemical analysis. Anal. Chem. **52**(9), 1445–1451 (1980). https://doi.org/10.1021/AC50059A017

[S50] C.A. Tolman, W.M. Riggs, W.J. Linn, C.M. King, R.C. Wendt, Electron spectroscopy for chemical analysis of nickel compounds. Inorg. Chem. **12**(12), 2770–2778 (1973). https://doi.org/10.1021/IC50130A006

[S51] S. Lars, T. Andersson, M.S. Scurrell, Infrared and ESCA studies of a heterogenized rhodium carbonylation catalyst. J. Catal. **59**(3), 340–356 (1979). https://doi.org/10.1016/S0021-9517(79)80003-2

[S52] J. Peeling, F.E. Hruska, D.M. McKinnon, M.S. Chauhan, N.S. McIntyre, ESCA studies of the uracil base. The effect of methylation, thionation, and ionization on charge distribution. Can. J. Chem. **56** (18) , 2405–2411 (1978). https://doi.org/10.1139/v78-393

[S53] M.C. Burrell, Y.S. Liu, H.S. Cole, An X-ray photoelectron spectroscopy study of poly(methylmethacrylate) and poly(α-methylstyrene) surfaces irradiated by excimer lasers. J. Vac. Sci. Technol. **4**(6), 2459–2462 (1986). https://doi.org/10.1116/1.574091

[S54] G.P. López, D.G. Castner, B.D. Ratner, XPS O 1s binding energies for polymers containing hydroxyl, ether, ketone and ester groups. Surf. Interface Anal. **17**(5), 267–272 (1991). https://doi.org/10.1002/sia.740170508

[S55] D.G. Castner, B.D. Ratner, Surface characterization of butyl methacrylate polymers by XPS and static SIMS. Surf. Interface Anal. **15**(8), 479–486 (1990). https://doi.org/10.1002/SIA.740150807

[S56] J. Szépvölgyi, A. Tüdös, I. Bertóti, X-ray photoelectron spectroscopy studies on solid xanthates. J. Electron Spectros. Relat. Phenomena **50**(2), 239–250 (1990). https://doi.org/10.1016/0368-2048(90)87068-Y

[S57] J. Russat, Characterization of polyamic acid/polyimide films in the nanometric thickness range from spin-deposited polyamic acid. Surf. Interface Anal. **11**(8), 414–420 (1988). https://doi.org/10.1002/sia.740110803

[S58] T. Sugama, L.E. Kukacka, N. Carciello, N.J. Hocker, Study of interactions at water-soluble polymer/$Ca(OH)_2$ or gibbsite interfaces by XPS. Cem. Concr. Res. **19**(6), 857–867 (1989). https://doi.org/10.1016/0008-8846(89)90098-7

[S59] L.C. Lopez, D.W. Dwight, M.B. Polk, The $\pi \rightarrow \pi^*$ shake-up phenomena in polyesters containing backbone aromatic groups. Surf. Interface Anal. **9**(1–6), 405–409 (1986).

[S60] J. Gardella, S.A. Ferguson, R.L. Chin, $\pi^* \leftarrow \pi$ shakeup satellites for the analysis of structure and bonding in aromatic polymers by X-ray photoelectron spectroscopy. Appl. Spectrosc. **40**(2), 224–232 (1986). https://doi.org/10.1366/0003702864509565

[S61] G.C. Allen, I.S. Butler, C. Kirby, Characterization of ferrocene and ($\eta^6$-benzene) tricarbonylchromium complexes by X-ray photoelectron spectroscopy. Inorg. Chim. Acta **134**(2), 289–292 (1987). https://doi.org/10.1016/S0020-1693(00)88098-6

[S62] K. Prabhakaran, C.N.R. Rao, Adsorption of carbonyl compounds on clean and modified Cu(110) surfaces: a combined eels-ups study. Appl. Surf. Sci. **44**(3), 205–210 (1990). https://doi.org/10.1016/0169-4332(90)90051-Z